

ANALYSIS OF THE $^{28}\text{Si}(p, \gamma)^{29}\text{P}$ REACTION DATA IN THE REGION OF THE SUBBARRIER SINGLE PARTICLE RESONANCES[†]

BY T. MATULEWICZ, P. DECOWSKI*, M. KICIŃSKA-HABIOR, B. SIKORA AND J. TÖKE**

Institute of Experimental Physics, Warsaw University***

(Received February 10, 1983)

The $^{28}\text{Si}(p, \gamma)^{29}\text{P}$ reaction data have been analysed in terms of a modified direct-semi-direct capture model which accounts for the presence of broad shape (single-particle) resonances in the entrance channel. Values of the spectroscopic factors for the ground state and 1.65 MeV and 2.88 MeV resonances in ^{29}P nuclei were extracted and found to be consistent with those obtained in other experiments. The modified theoretical analysis scheme was found to provide a convenient tool for analysing the radiative capture reaction data.

PACS numbers: 25.40.-h

1. Introduction

Direct radiative proton capture reaction has proved in the past its usefulness as a tool of nuclear spectroscopy at low incident energies [1–5]. In an ideal case, when all non-direct reaction channels can be disregarded, the ratio of the measured radiative capture reaction cross section to the theoretical one is equal to the proton spectroscopic factor of the final state, a physical quantity of paramount importance. Unfortunately, in most cases it is not possible to avoid other reaction mechanisms, extraction of spectroscopic factors becomes a real problem and analysis schemes must be devised which take those other mechanisms into account as well.

A modification of the theoretical analysis scheme of the dipole radiative proton capture reaction data has been proposed recently [6] which offers a relatively simple way of overcoming the most severe problems of the data analysis caused by the presence of broad shape resonances and the non-negligible semidirect amplitudes. The new analysis scheme treats the direct capture and the capture via those broad resonances on equal basis in the framework of the direct-semidirect capture model. This results not only in a noticeable

[†] Financial support under Project 04.3 is gratefully acknowledged.

* Present address: KFA Jülich, W. Germany.

** Present address: GSI Darmstadt, W. Germany.

*** Address: Instytut Fizyki Doświadczalnej, Uniwersytet Warszawski, Hoża 69, 00-681 Warszawa, Poland.

simplification with respect to the conventional combined direct-semidirect plus R-matrix analysis scheme but supposedly allows also to avoid some major ambiguities of the latter. The main novelty of the new scheme consists in using a special energy-dependent single-particle potential for generating the relative motion wave function in the entrance channel i.e. the scattering wave function. This potential allows to generate scattering state wave functions with correct phase shifts in the region of isolated resonances and thus accounts for effects of coupling of single-particle continuum states with the more complex structured states — the bound states embedded into the continuum (BSEC). The coupling of the incoming wave with states having large El widths (and thus contributing to the observed gamma yield via the semidirect amplitude) is accounted for by renormalizing appropriately the dipole effective charge.

In the present paper the existing experimental data on the excitation functions and angular distributions of the $^{28}\text{Si}(p, \gamma)^{29}\text{P}$ reaction in the proton energy range of 1.5–3.0 MeV [5, 7] are reanalysed in terms of the new analysis scheme. This serves two goals. First of all, the applicability of the new approach is being tested and its possible limitations are studied and secondly, the spectroscopic information concerning the ground and first excited state as well as the shape resonances in the phosphorus nuclei is being reassessed.

A preliminary report on this analysis was presented in [8].

2. Analysis and results

The proposed analysis scheme is based on the formula for the direct proton capture cross section derived in [1]:

$$\sigma = \text{const (phase space factor)} S |\langle u(r) | O_{E1}(r) e_{\text{eff}}(r) | \chi(r) \rangle|^2, \quad (1)$$

where S denotes the spectroscopic factor of the final state, $\chi(r)$ denotes the relative wave function of the proton-target system in the entrance (continuum) channel, $u(r)$ is the proton bound state wave function in the final nucleus, O_{E1} is the electric dipole operator, e_{eff} denotes proton effective dipole charge.

In this formula special attention has been paid to two quantities — the continuum wave function $\chi(r)$ which might be made responsible for the resonant behaviour of the reaction amplitude and the effective charge e_{eff} which has to account for the presence of the semidirect reaction path.

The $^{28}\text{Si}(p, \gamma)$ reaction excitation function exhibits two broad resonances in the proton energy range of 1.5–3.0 MeV — one at 1.65 MeV ($J = 3/2^-$, $\Gamma = 52$ keV) and other at 2.88 MeV ($J = 1/2^-$, $\Gamma = 400$ keV). Those resonances can be regarded as the two spin components of the 2p proton wave shape resonance and accordingly they could be used to determine the single-particle potential depth and the strength of the spin-orbit force in the reaction entrance channel (see Fig. 1).

The fact that those resonances are not pure single-particle ones becomes clear when comparing their measured widths with the theoretical single-particle widths and it has an explanation in the coupling of pure single-particle continuum states with the BSEC. In order to account for the effects of this coupling in the present analysis the energy depend-

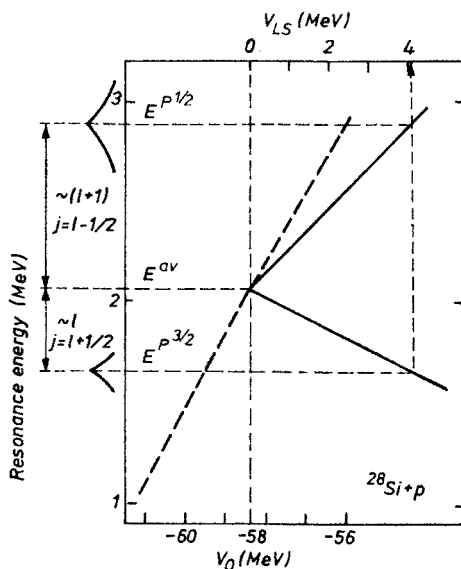


Fig. 1. Energies of the p-wave single particle resonances as functions of the depth of the real potential well and the strength of the spin-orbit interaction. The tilted dashed line corresponds to the no-spin-orbit case and thus predicts the position of the centroid of the $p_{1/2}$ and $p_{3/2}$ resonances as a function of the real well depth. The two solid lines illustrate the spin-orbit splitting as a function of the strength of the LS potential at the fixed real potential depth

ent effective potential approach from [9] has been employed. As it was shown in [9], a variation of the single particle potential accordingly to the formula:

$$U_{\text{eff}}(E) = U_0 + \sum_{i=1}^N \frac{\gamma}{E - \varepsilon_i} \quad (2)$$

results in splitting a single particle resonance into $N+1$ resonances while preserving the total single particle strength. Widths and positions of those $N+1$ resonances are functions of the parameters U_0 , γ_i^2 and ε_i which are treated as adjustable ones.

The effect of the energy dependence (2) can be understood from Fig. 2 which is borrowed from [9] and which assumes $N = 1$. The almost straight line in Fig. 2b labelled $U_{\text{res}}(E)$ describes the dependence of the energy of a hypothetical single-particle resonance for a particular partial wave on the well depth. Variation of the well depth with the particle energy (Fig. 2b) produces shape resonances at two different energies (Fig. 2c) at which the effective potential depth and the resonance-adjusted depth are equal to each other, i.e. there, where $U_{\text{eff}}(E) = U_{\text{res}}(E)$. Clearly the relative motion wave functions in those two resonances have equal numbers of nodes and thus represent fragments of one pure single-particle resonance from Fig. 2a. In [9] it has been shown that in such a fragmentation the total single-particle strength is conserved.

Insertion of the single-particle wave function generated by applying the effective potential approach into the standard formula (1) for the direct radiative capture amplitude

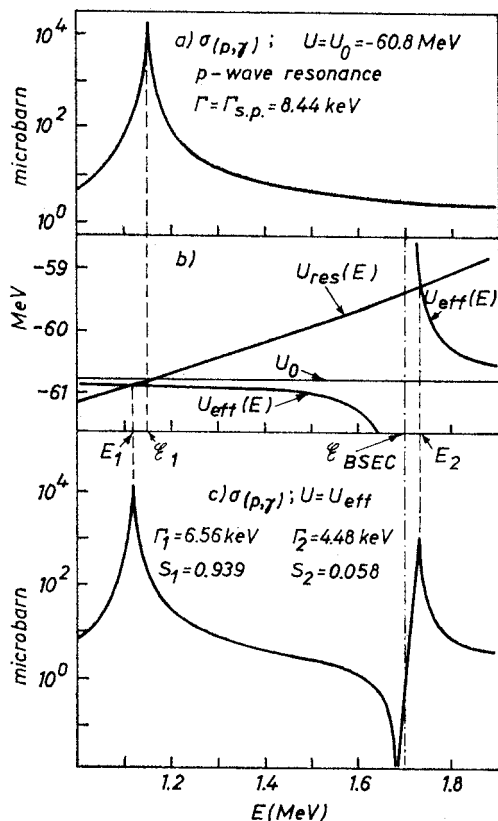


Fig. 2. Excitation function for the (p, γ) reaction on a hypothetical $A = 28$ $Z = 14$ nucleus generated by using in the entrance channel a constant depth potential (upper section) and the energy dependent effective potential with $U_{\text{eff}}(E)$ shown in the middle section (lower section). The $U_{\text{res}}(E)$ line in the middle section represents the dependence of the single-particle resonance energy on the well depth for a particular well geometry

allows to treat the capture via single-particle resonances on equal footing with the direct capture. The obtained amplitude represents the sum over these two ways of capture and thus there is no longer need to resort to the R -matrix calculus as far as the (broad) single-particle resonances are concerned. On the other hand, as far as the narrow compound nucleus resonances are concerned, their contribution to the measured yield can be made negligible, when the incident energy is appropriately chosen. As a consequence, the use of the R -matrix approach can in many cases be avoided at all.

In the present analysis of the radiative capture reaction data also the semidirect mechanism [10–12] has been accounted for. This was done by renormalizing appropriately the effective dipole charge of the proton:

$$e_{\text{eff}}(r) = e + \delta e_{\text{pol}}(r), \quad (3)$$

where e is the absolute value of proton charge. The polarization charge was assumed to be composed of two parts:

$$\delta e_{\text{pol}}(r) = -0.5e + eq(E)f(r). \quad (4)$$

The first term merely accounts for the recoil of the $A = 2Z$ target nucleus. The second one accounts for the coupling of the entrance channel wave function to the GDR of the final nucleus (built on the state being studied). Its energy dependence is determined by the GDR strength function and was assumed to be given by the simple formula $q(E) = q_0 \Gamma_{\text{GDR}}/2 \times [(E_\gamma - E_{\text{GDR}})^2 + \Gamma_{\text{GDR}}^2/4]^{-1/2}$.

As far as the radial dependence of the polarization charge is concerned two different types of formfactors have been tested — the Saxon-Woods one and the surface peaked one. None of them was here, however, found as being more favorable than the other one. It is worth pointing out that the polarization charge (4) affects only weakly the resonance width which is clearly helpful when carrying out the theoretical analysis. On the other hand its effect on the magnitude of the cross section is significant and may lead to errors in extracted values of the spectroscopic factors when the energy range covered by the experiment is not sufficiently large.

Theoretical fits to the $^{28}\text{Si}(p, \gamma_0)$ and to the $^{28}\text{Si}(p, \gamma_1)$ reaction excitation functions and angular distributions have yielded the following energy dependent potential parameters: $U_0 = -57.60$ MeV, $V_{1s} = 4.06$ MeV, $r_0 = 1.3$ fm, $a = 0.5$ fm as the common values for both $3/2^-$ and $1/2^-$ components and $\epsilon_1(3/2^-) = 3.31$ MeV, $\gamma_1^2(3/2^-) = 1.29$ MeV, $\epsilon_1(1/2^-) = 3.46$ MeV, $\gamma_1^2(1/2^-) = 0.581$ MeV. The last four parameters are to be interpreted as the positions and appropriate coupling strengths of the BSEC which couple to the two dominant partial waves in the entrance channel.

In the case of the $^{28}\text{Si}(p, \gamma_0)$ reaction, experimental data cover a sufficiently large energy range to allow simultaneous determination of both the spectroscopic factor and effective charge parameters. The fits shown in Fig. 3 correspond to $S = 0.36$, $E_{\text{GDR}} = 19.0$ MeV, $\Gamma_{\text{GDR}} = 3.8$ MeV (see [13]), $q_0(3/2^-) = 7.1$ and $q_0(1/2^-) = 8.9$. The extracted value of the spectroscopic factor, the uncertainty of which we estimate on 20%, agrees well with the data from other experiments (see Table I).

TABLE

Spectroscopic factors for the ground and first excited states of the ^{29}P nucleus

$E_x = 0$ MeV ($1/2^+$)	$E_x = 1.383$ MeV ($3/2^+$)	Reaction	Reference
0.50	0.59	theory	[14]
0.36		$^{28}\text{Si}(p, \gamma)$	this work
0.36	0.50	$^{28}\text{Si}(p, \gamma)$	[5]
0.45		$^{28}\text{Si}(p, \gamma)$	[7]
0.45	0.23	$^{28}\text{Si}(^3\text{He}, d)$	[15]
0.52-0.60	0.41-0.59	$^{28}\text{Si}(^3\text{He}, d)$	[16]
0.54	0.78	$^{28}\text{Si}(^3\text{He}, d)$	[17]
0.46	0.64	$^{28}\text{Si}(^3\text{He}, d)$	[18]
0.65	0.88	$^{28}\text{Si}(^3\text{He}, d)$	[19]
0.51	0.90	$^{28}\text{Si}(^3\text{He}, d)$	[20]
0.21	0.21	$^{28}\text{Si}(^3\text{He}, d)$	[21]
0.15		$^{28}\text{Si}(^3\text{He}, d)$	[21]
0.50		$^{28}\text{Si}(^3\text{He}, d)$	[21]
0.50	0.71	$^{28}\text{Si}(^3\text{He}, d)$	[22]
0.59	0.37	$^{28}\text{Si}(\alpha, t)$	[23]

In the case of the $^{28}\text{Si}(p, \gamma_1)$ reaction, the quality of the available experimental data (relatively large statistical errors combined with the narrow width of the covered energy range) is too low to allow the simultaneous determination of all the parameters involved with an acceptable accuracy. Therefore in this case we renounce from an independent extraction of the spectroscopic factor, assuming for it the value of 0.5 consistent with

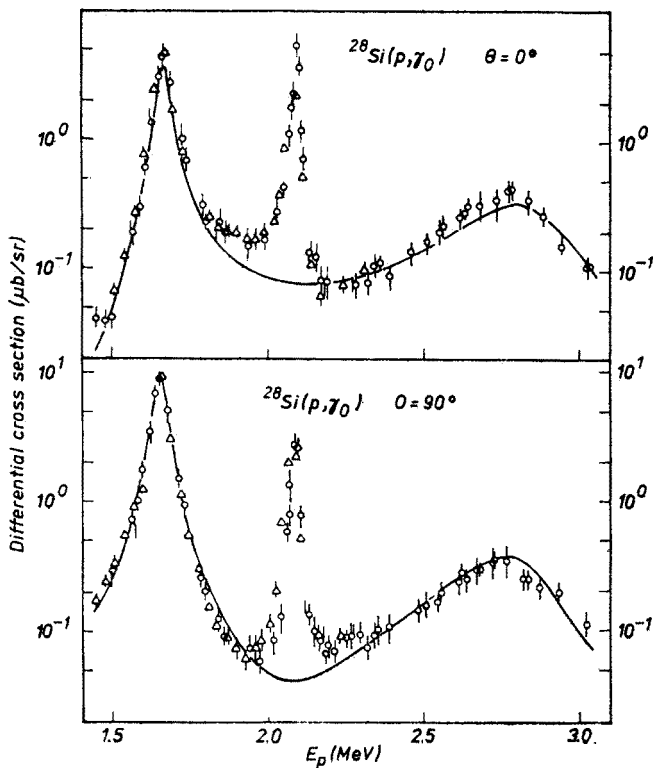


Fig. 3. Comparison of the experimental excitation functions of the $^{28}\text{Si}(p, \gamma_0)^{29}\text{P}$ reaction with theoretical predictions (solid lines) for the E1 capture from the $p_{3/2}$ and $p_{1/2}$ states. Resonance seen at 2.1 MeV has $J = 1/2^+$ and thus is not taken into account in the calculations (M1 transition). Note that this resonance produces interference yield at 0° but not at 90° as expected for E1 end M1 transitions

other experimental data (see Table I). With this value of 0.5, the effective charge parameter q_0 which characterizes the coupling strength to the GDR built on the first excited state of the ^{29}P nucleus is found to assume values $q_0(3/2^-) = 17.9$ and $q_0(1/2^-) = 23.7$. The resulting fits to the experimental data are shown in Fig. 4 by solid lines. In the same figure dashed lines present best fits obtained when both the spectroscopic factor and the effective charge parameters were allowed to vary. These fits correspond to a considerably lower value of the spectroscopic factor $S = 0.1$ which suggests that the quality of experimental data is here indeed inadequate for simultaneous and accurate determination of all the parameters involved.

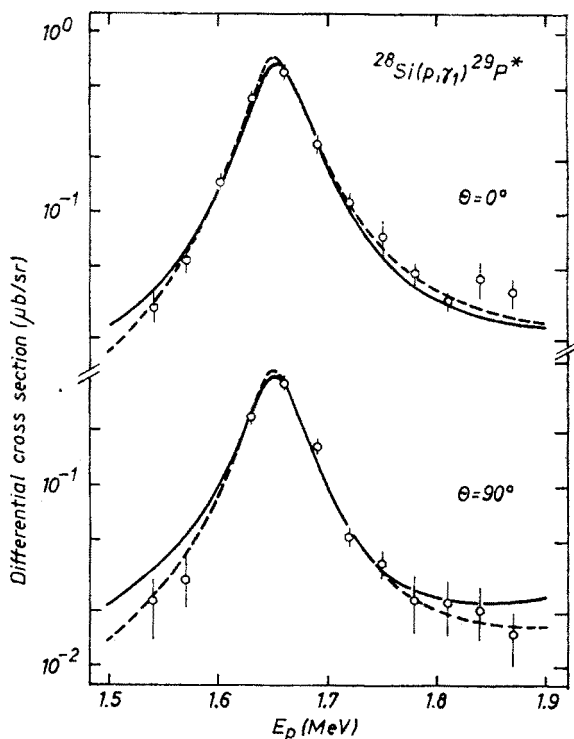


Fig. 4. Comparison of the experimental excitation functions of the $^{28}\text{Si}(p, \gamma_1)^{29}\text{P}^*$ reaction with theoretical predictions. Solid lines correspond to the fixed value of the spectroscopic factor $S = 0.5$, while the dashed lines represent the best fits obtained when also the S -value was allowed to vary.

Theoretical fits to the excitation functions at 0° and 90° shown in Figs. 3 and 4 correspond to the spectroscopic factors for the observed $3/2^-$ and $1/2^-$ shape resonances $S_p(3/2^-) = 0.85$ and $S_p(1/2^-) = 0.66$.

3. Discussion

The new analysis scheme for the radiative capture reaction data proved here to be a convenient tool for extracting the spectroscopic information both on bound and resonant states of nuclei. Depending on the quality of the experimental data two different approaches have to be adopted. In cases, when the experimental data have an adequate quality, a self-contained analysis is possible which yields the values of the spectroscopic factors and of the effective charge parameters involved. In cases, when the quality of the experimental data is rather poor, the results of the simple fitting have large uncertainties. In such cases some parameters have to be fixed based on other experimental results. It is worth pointing out that this should not be considered as a deficiency of the new analysis scheme as compared to the conventional one which sets requirements to the quality of the experimental data as well.

The fact that the new scheme allows us to fit the experimental data in a broad energy range, makes it especially suitable for predicting — by extrapolating theoretically from experiments at higher energies — the capture yields at the astrophysical energies where the experiments are difficult to carry out.

We want to thank Professor Z. Wilhelmi for his kind interest and continuous support of this work.

REFERENCES

- [1] C. Rolfs, *Nucl. Phys.* **A217**, 29 (1973).
- [2] C. Rolfs, R. E. Azuma, *Nucl. Phys.* **A227**, 291 (1974).
- [3] C. Rolfs, W. S. Rodney, M. H. Shapiro, H. Winkler, *Nucl. Phys.* **A241**, 460 (1975).
- [4] H. P. Trautvetter, C. Rolfs, *Nucl. Phys.* **A242**, 519 (1975).
- [5] F. Terrasi, A. Brondi, P. Cuzzocrea, R. Moro, M. Romano, *Nucl. Phys.* **A324**, 1 (1979).
- [6] J. Töke, P. Decowski, B. Sikora, NPL Annual Report, Warsaw 1979, p. 21.
- [7] M. Modirnia, PhD Thesis, University of Bordeaux 1976.
- [8] J. Cseh, M. Dąbrowska, P. Decowski, W. Grochulski, P. Jaracz, M. Kicińska-Habior, T. Matulewicz, B. Sikora, E. Somorjai, J. Töke, NPL Annual Report, Warsaw 1980, p. 9, 14.
- [9] J. Töke, T. Matulewicz, to be published.
- [10] C. F. Clement, A. M. Lane, J. R. Rook, *Nucl. Phys.* **66**, 273 (1965).
- [11] G. Longo, F. Saporetti, *Nuovo Cimento* **56B**, 264 (1968).
- [12] J. Zimanyi, I. Halpern, V. A. Madsen, *Phys. Lett.* **33B**, 205 (1970).
- [13] C. R. Lamontagne, B. Frois, R. J. Slobodrian, H. E. Conzett, Ch. Leemann, *Z. Phys.* **A295**, 55 (1980).
- [14] B. H. Wildenthal, J. McGrory, *Phys. Rev.* **C7**, 714 (1973).
- [15] A. Djaloeis, S. Gopal, J. Bojowald, W. Oelert, N. G. Puttaswamy, P. Turek, C. Mayer-Boricke, *Phys. Rev.* **C26**, 797 (1982); S. Gopal, private communication.
- [16] M. Matsuoka, K. Hatanaka, M. Fujiwara, Y. Fujita, T. Saito, K. Hosono, A. Shimizu, M. Kondo, F. Ohtani, H. Sakaguchi, A. Goto, N. Nakanishi, Y. Toba, *Nucl. Phys.* **A373**, 377 (1982).
- [17] K. Koyama, N. Nakanishi, S. Takeda, S. Yamada, H. Sakaguchi, M. Nakamura, S. Takeuchi, H. Ohnuma, *J. Phys. Soc. Japan* **43**, 755 (1977).
- [18] L. Ray, W. R. Coker, *Phys. Rev.* **C13**, 1367 (1976).
- [19] W. E. Dykoski, D. Dehnhard, *Phys. Rev.* **C13**, 80 (1976).
- [20] R. J. Peterson, R. A. Ristinen, *Nucl. Phys.* **A246**, 402 (1975).
- [21] P. Leleux, P. C. Macq, J. P. Meulders, C. Pirart, *Z. Phys.* **271**, 139 (1974).
- [22] H. Ejiri et al., *J. Phys. Soc. Japan* **21**, 2110 (1966).
- [23] C. R. Bingham, R. J. de Meijer, L. W. Put, J. C. Vermeulen, D. Dijkhuizen, KVI Groningen Annual Report 1976, p. 19.